Attenuation Assessment for NDT of Austenitic Stainless Steel Welds

Marie-Aude PLOIX, Philippe GUY, GEMPPM - INSA Lyon, Villeurbanne, France
Rachid EL GUERJOUMA, LAUM, Le Mans, France
Joseph MOYSAN, Gilles CORNELOUP, LCND, Aix-en-Provence, France
Bertrand CHASSIGNOLE, EDF R&D, Moret-sur-Loing, France

Abstract. Multipass welds made in 316-L stainless steel are specific welds of primary circuit in nuclear power stations. Their complex structure complicates ultrasonic assessment of their structural integrity : they present a heterogeneous anisotropy that deteriorates the propagation of waves (deviation and division of the beam, attenuation…). Polycrystalline materials as stainless steel are composed of numerous discrete grains whose elastic properties are anisotropic and crystallographic axes are differently oriented.

When an acoustic wave propagates through such a material, it is attenuated by scattering at grain boundaries. Provided the elastic constants of the different homogeneous domains of the weld, the finite-element model *ATHENA* (EDF & INRIA) predicts path and velocity of ultrasonic waves, but attenuation has still to be integrated into the code. Our work aims to provide realistic input data of attenuation compatible with the existing model in studying mechanisms leading to attenuation in anisotropic structures. The value of this attenuation depends on the size, shape, orientations distribution and anisotropy of the grains. When grains are equiaxed and randomly oriented, the average elastic properties are isotropic. But in the case of multipass welds made of austenitic stainless steel, crystalline growth mechanisms acting during the solidification lead to a macroscopic texture, with elongated and preferentially oriented grains. Thus their structure is anisotropic, and ultrasonic attenuation is a function of the propagation direction.

First, experimental ultrasonic measurements obtained by means of classical techniques are presented and compared with theoretical predictions of the literature. Then other experimental data obtained by mapping the incident and transmitted ultrasonic fields are compared with modelling based on the plane waves angular spectrum decomposition of the beam in order to evaluate the energy loss experienced by each plane wave component of the beam.

Introduction

The assessment of the structural integrity of an austenitic stainless steel weld requires a good understanding of the waves propagation within the structure. These welds are polycrystalline materials composed of elongated anisotropic grains whose crystallographic axes are differently oriented. Indeed crystalline growth mechanisms acting during the solidification of the weld lead to a macroscopic texture with elongated and preferentially oriented grains [1]. An acoustic wave propagating through such a material can be deviated and strongly attenuated.

In order to do well defined ultrasonic weld non-destructive testing, we need to better understand the propagation in such a medium. In this aim, a 2D finite-element model called *ATHENA* is developed by INRIA and EDF. This model simulates ultrasonic propagation in anisotropic and heterogeneous elastic structures [2][3]. For this simulation, the weld is

described as a set of homogeneous and orthotropic subdomains with their own elastic properties, i.e. crystallographic orientations and disoriented elasticity tensor (cf. Figure 1).
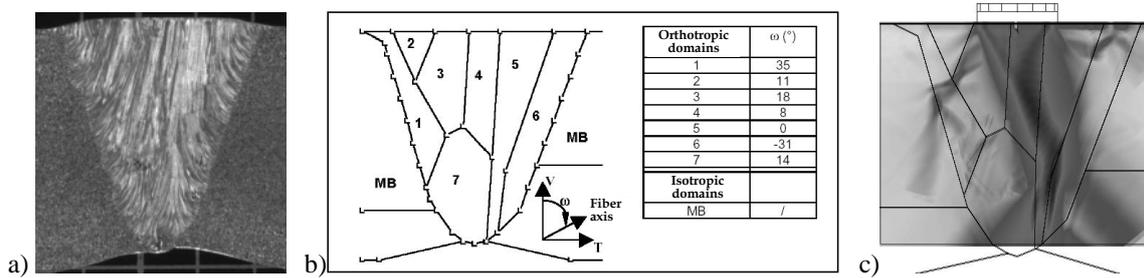
Figure 1. (a) Macrograph of an industrial weld (D717A), (b) Description in homogeneous orthotropic subdomains, (c) Simulation of propagation.

Experimental results prove that the simulation provides a good prediction of the wave propagation in terms of beam description (particularly deviations and divisions) [4]. But amplitudes collected are not representative of real measurements insofar as an intrinsic attenuation model and realistic values are still missing [5]. Figure 2 shows an example of the difference between experimental and modelling attenuation values for different incidence configurations.
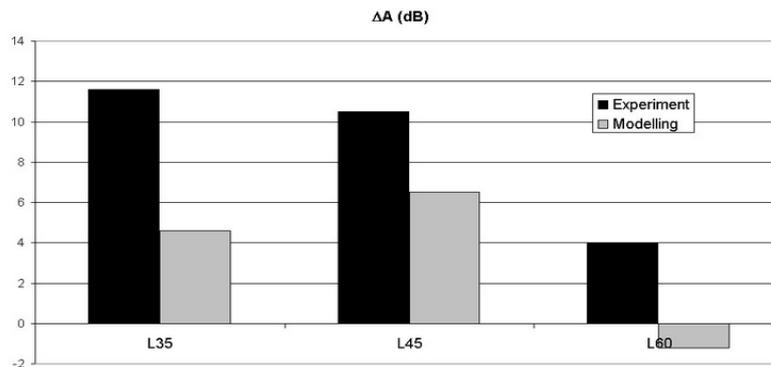
Figure 2. Values of attenuation gap between modelling and experiment for three propagation angles [5].

Attenuation in such materials is mainly caused by scattering at grain boundaries. The value of this attenuation depends on several distributions : size, shape and orientations of the grains but also on their anisotropy. This work aims at studying ultrasonic attenuation as a function of the grain orientation. We first present a classical measurement setup and compare results to theory. Then another approach based on the beam decomposition into plane waves angular spectrum is presented.
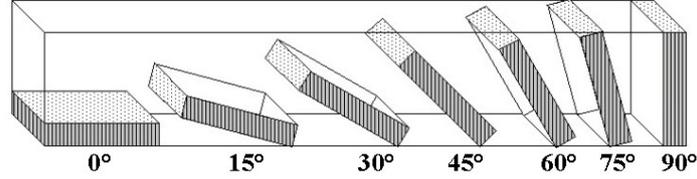
1. Description of the Samples

The welded samples used for the longitudinal wave attenuation measurements were cut in a flat position and shielded metal arc welding mock-up in such a way that samples are macroscopically homogeneous and orthotropic. Table 1 details the composition of the filling metal (AISI 316L steel) used to elaborate these welds.

Table 1. Composition of filling metal for welding mock-ups.

Element	Cr	Ni	Mo	Mn	Si	Cu	Co	C	P	S
Content (%)	19.8	11.9	2.34	1.9	0.41	0.07	0.056	0.03	0.01	0.001

As far as we want to determine ultrasonic attenuation versus grain orientation, the mock-up was cut into samples from 0 to 90° at 15° increments, as shown by Figure 3. This allows us to stay at normal incidence. Indeed oblique incidence complicates considerably measurements because of the mode conversions and the beam aperture. Because of the cut difficulties, the real orientations that are used in the following are 0°, 10°, 35°, 45°, 60°, 80° and 85°.


Figure 3. Scheme of the samples cut-out according to the grain orientation.

2. Classical Technique of Measurement

2.1. Setup and Computations

A schematic representation of the experimental setup is shown on Figure 4. It is composed by two broadband transducers (an emitter Ø0.5" and a receiver Ø0.75" with 2.25MHz central frequency) immersed in water. The principle consists in registering two signals in transmission mode [6]. A first acquisition is performed in water and provides the reference signal $r(t)$. The second signal $s(t)$ is acquired after having inserted the sample between and parallel to the both transducers.
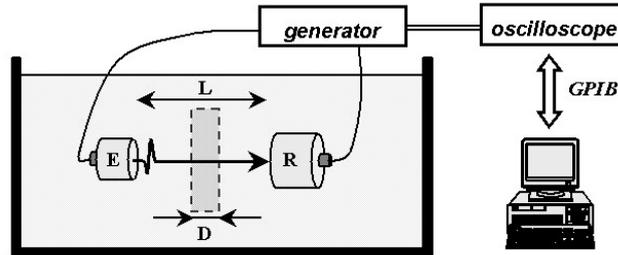
Figure 4. Experimental setup.

Phase velocity and attenuation dispersions, $V(f)$ and $\alpha(f)$, can then be calculated by computing Fourier transforms $R(f)$ and $S(f)$ of the two temporal signals and then applying the following relationships :

$$V(f) = \frac{V_{water}}{1 + \frac{\Delta\varphi(f)V_{water}}{2\pi f D}} \qquad \text{and} \qquad \alpha(f) = \frac{1}{D}\left(ln\, T(f) - ln\, \left|\frac{S(f)}{R(f)}\right| \right) + \alpha_{water}$$

where D is the thickness of the sample, V_{water} is the phase velocity in water (considered constant for a given temperature [7]), $\Delta\varphi(f)$ is the unwrapped phase shift between the two signals, α_{water} is the attenuation in water (negligible) and $T(f)$ is the total transmission coefficient in normal incidence :

$$T(f) = \frac{4\rho_{water}V_{water}\rho V(f)}{(\rho_{water}V_{water} + \rho V(f))^2}$$

with ρ and V represent the density and the phase velocity respectively.

## 2.2. Results and Comparison to Theory

2.2.1. Phase Velocity

Phase velocity dispersion was calculated for each grain orientation of the samples with the formula previously given. Figure 5 shows the dispersion curves and the behaviour of the phase velocity at a fixed frequency (2.25MHz) as a function of the grain orientation.

Velocities on the left figure present very small fluctuations versus frequency. So the material is weakly dispersive in the point of view of phase velocity. On the other hand curves show a great difference of values according to the grain orientation.

This is clearer on the right side figure. Velocity values increase from 0° to 45° and then decrease until 90° with a maximum gap of around 700m/s. This behaviour is typical from the assumption of orthotropic material.

A theoretical curve is also plotted on the right side figure. It was calculated from the elastic constants of the material determined in a previous study [4] from velocities measurement with a similar setup. We can see that experimental and theoretical values are in good agreement.
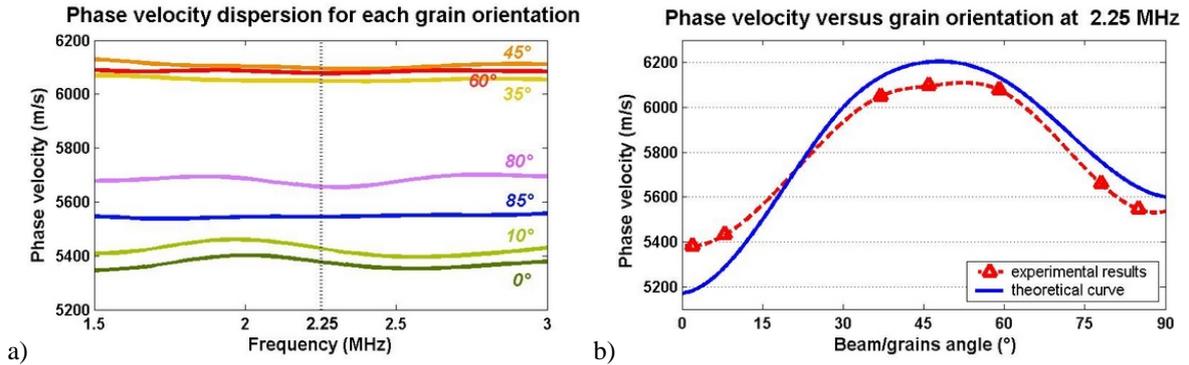

Figure 5. Phase velocity results : (a) versus frequency, (b) versus grain orientation at 2.25MHz.

2.2.2. Attenuation

Figure 6 presents the experimental results in attenuation. Dispersion curves are globally increasing with frequency. However some curves show oscillations that are not physically coherent. This can be due to the fact that measurements are made in the near field of the emitter or because of the deviation of the beam in going through the material… The problem is still under consideration.

Experimental values of the literature on similar material confirm that our results are in the right order of magnitude [8]. Some theoretical models predict that the scattering attenuation in textured polycrystals should increase continuously versus the grain orientation [9][10]. Our experimental results show a good agreement with these models from 45° to 90° grain orientation, but not for lower angles.
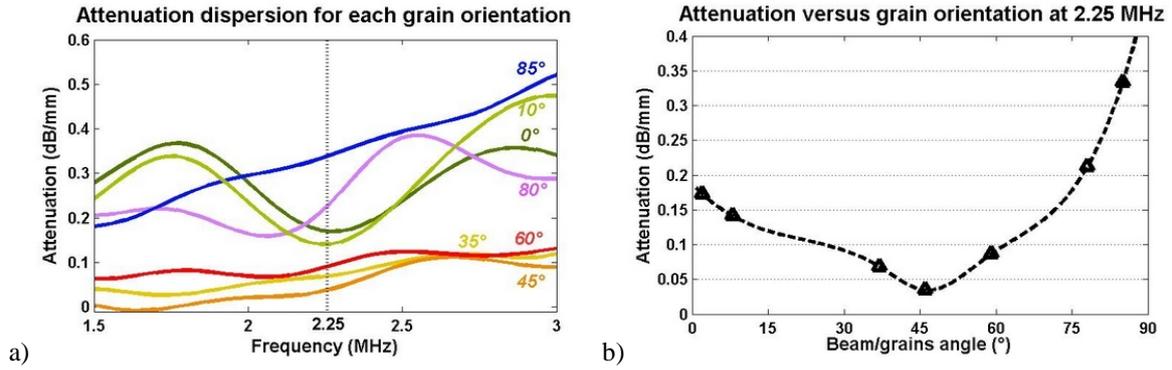
Figure 6. Attenuation results : (a) versus frequency, (b) versus grain orientation at 2.25MHz.

Seldis and Pecorari [8] found a behaviour of the measured attenuation similar to ours with the same setup. They propose another approach that provided them a curve in agreement with theory. This latter method based on the angular plane waves spectrum decomposition of the beam is interesting because it allows to take into account the mode conversions, the deviation and the structure of the beam.

Then we developed a similar setup and treat the data to determine intrinsic attenuation by a process based on some elements presented in their publication.

3. Experimental Approach Based on Beam Decomposition

3.1. Experimental Setup and Signal Processing

The immersion setup is described in Figure 7. It is composed by an emitting transducer (Ø0.5" with 2.25MHz central frequency) and a hydrophone as receiver (Ø0.5mm). The location of the sample is in the farfield of the emitter.
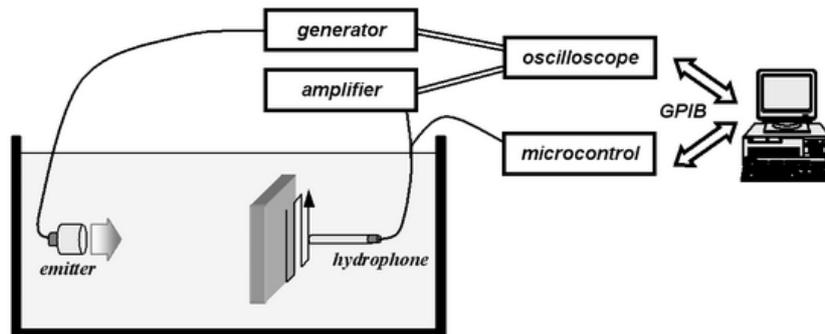

Figure 7. Experimental setup.

The hydrophone scans a plane $z=z_o$ parallel to the emitter face and acquires a signal $s(t,x,y,z_o)$ at each point (x,y) of the plane. The angular frequency spectrum $S(x,y,\omega,z_o)$ is obtained for each time signal by Fourier-transform. For a given angular frequency ω_o, a 2D spatial Fourier-transform gives the so called plane waves angular spectrum $U(k_x,k_y,\omega_o,z_o)$ in the k-space domain.

In our experiments, two different planes are scanned. First the incident field is mapped without any sample. The hydrophone moves in the plane containing the front face of the sample ($z_o=0$). Then the sample is inserted and the transmitted field is mapped in a plane in the proximity of the sample's back face ($z_o>d$). For the angular frequency ω_o

corresponding to a frequency of 2.25MHz, the plane waves angular spectra $U_{inc}(k_x,k_y,\omega_o,z_o)$ and $U_{tra}(k_x,k_y,\omega_o,z_o)$ are calculated.

A quasi-theoretical transmitted plane waves angular spectrum $U'_{tra}(k_x,k_y,\omega_o,z_o)$ is obtained by multiplying $U_{inc}(k_x,k_y,\omega_o,z_o)$ (cf. Figure 8a) with the transmission coefficients calculated in the k-space domain (example on Figure 8b).
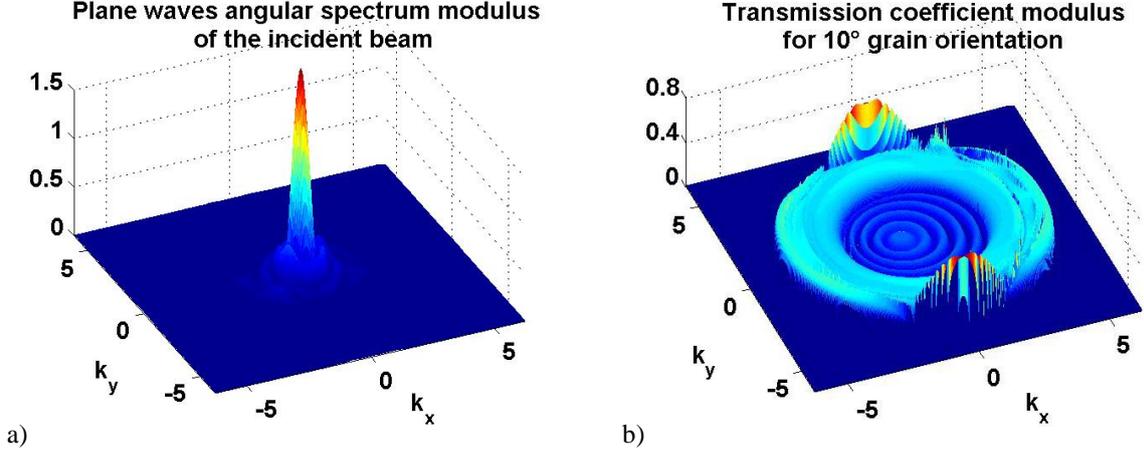
Figure 8. Plane waves angular spectrum modulus : (a) incident beam, (b) transmission coefficient (10°).

Transmission coefficients are obtained by solving the Christoffel equation with the corresponding boundary conditions at each interface. These calculations are performed for each incidence direction of a plane wave.

Moreover the problem of transmission coefficients computation was first solved in the orthotropic case [11] and was then extended to the monoclinic case. Indeed the elastic description of an orthotropic material disorientated according to an axis of the fixed coordinate system becomes monoclinic. So samples with 0° and 90° grain orientation present an orthotropic description whereas the others have a monoclinic one. We note however that the number of independent elastic constants keeps the same (9 for orthotropic material). The new 13 constants of the monoclinic case are linear combinations of the initial 9 ones.

In this modelling, deviations and mode conversions are then taken into account. The only phenomenon that is not counted is intrinsic attenuation of the material. The attenuation for each direction of propagation (k_x,k_y) is then given by :

$$\alpha(k_x, k_y, \omega_0, z_0) = \frac{20}{d} \, log\left(\frac{\left|U'_{tra}(k_x, k_y, \omega_0, z_0)\right|}{\left|U_{tra}(k_x, k_y, \omega_0, z_0)\right|} \right)$$

where d is the sample width.
The beam attenuation is derived from the following relationship :

$$\alpha_{beam}(\omega_0) = \frac{10}{d} \, log\left(\frac{E'_{tra}(\omega_0)}{E_{tra}(\omega_0)} \right)$$

where the energies E_{tra} and E'_{tra} are defined by :

$$E_{tra}(\omega_0) = \iint \left|U_{tra}(k_x, k_y, \omega_0)\right|^2 dk_x dk_y$$

$$E'_{tra}(\omega_0) = \iint \left|U_{inc}(k_x, k_y, \omega_0)\right|^2 T^2_{ws}(k_x, k_y, \omega_0) T^2_{sw}(k_x, k_y, \omega_0) dk_x dk_y$$

T_{ws} and T_{sw} are the transmission coefficients defined in the k-space domain at the first and the second interface of the sample respectivly.

3.2. First Results and Discussion

Beam attenuation bas been calculated from the previous relationships. Experimental results are presented in Figure 9 where attenuation at 2.25MHz is plotted versus grain orientation.

Attenuation curve shows increasing values from 0° to 30°, then it is rather constant until 60° and finishes with an increase until 90°. We can also observe that attenuation values are greater than one measured by the means of the classical setup. These results do not yet agree in a satisfactory way with theoretical predictions and are moreover quite different from the previous results.
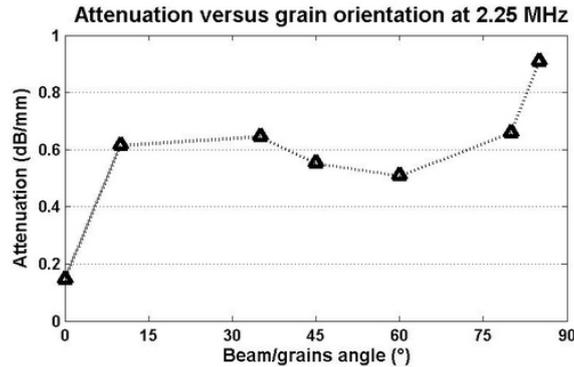
Figure 9. Experimental attenuation versus grain orientation at 2.25MHz.

Several elements that can explain these observations are still on study. First we noted that an effect of near field of the grains exists and has to be taken into account in the measurements. Secondly the superposition of the plane wave and the edge wave classically generated by a baffled piston has still to be analysed [12]. It has to be noted that this problem also exists in the classical method decribed in the first part of this paper. The superposition of the geometrical and the edge waves are probably responsible of the fluctuations observed in the spectra of Figure 6a.

Conclusions

Intrinsic attenuation is a mechanism difficult to qualify and still more difficult to quantify. Attenuation measurement particularly interested numerous authors until now. But neither universal technique nor universal table of attenuation values exist.

In this paper we presented the classical immersion technique and compared experimental results to theoretical behaviours predicted by Hirsekorn and Ahmed's theories. We found that the curves do not completely agree with these theories especially for weak angles.

So a second approach was dealt with. It is based on the decomposition of the beam into plane waves angular spectrum and on the application of the transmission coefficients in the k-space domain on the incident beam. The preliminary measurements carried out with this second approach result in higher values than with the first setup. But they nevertheless seem to present a behaviour more close to the one theoritically predicted.

At this stage, it is difficult to say, if the observed discrepancy between experimental results and theory are due to the measurement processes or if some hypotheses of the theoretical models are not fulfilled by our samples. As described in the literature [12], attenuation measurement is very sensitive to numerous parameters of the setup and they have still to be deeply analysed.

Yet this result allow to provide input data to perform first simulations with *ATHENA* code.

References

[1] MOYSAN J., APFEL A., CORNELOUP G. & CHASSIGNOLE B., *Modelling the Grain Orientation of Austenitic Stainless Steel Multipass Welds to Improve Ultrasonic Assessment of Structural Integrity*, International Journal of Pressure Vessels and Piping, Vol. 80, pp. 77-85 (2003).

[2] SCHUMM A. et al., *Numerical Modelling of the Structural Noise in Welds*, submitted to 9th European Conference on NDT, Berlin (2006).

[3] BECACHE E., JOLY P. & TSOGKA C., *An Analysis of New Mixed Finite Elements for the Approximation of Wave Propagation Problems*, SIAM Journal on Numerical Analysis, Vol. 37, pp. 1053-1084 (2000).

[4] CHASSIGNOLE B., VILLARD D., DUBUGET M., BABOUX J.-C. & EL GUERJOUMA R., *Characterization of Austenitic Stainless Steel Welds for Ultrasonic NDT*, Review of Progress in QNDE, Vol. 20, pp. 1325-1332 (2000).

[5] CHASSIGNOLE B., DUPOND O., SCHUMM A., FOUQUET T. & MOYSAN J., *Ultrasonic Modelling of Austenitic Stainless Steel Welds : Improvement in the Comprehension of Anisotropic and Heterogeneous Structure Effects*, 4th ICNDE London, pp. 910-918 (dec. 2004)

[6] HE P., *Direct Measurement of Ultrasonic Dispersion Using a Broadband Transmission Technique*, Ultrasonics, Vol. 37, pp. 67-70 (1999).

[7] DEL GROSSO V.A. & MADER C.W., *Speed of Sound in Pure Water*, Journal of the Acoustical Society of America, Vol. 52, No. 5, pp. 1442-1446 (1972).

[8] SELDIS T. & PECORARI C., *Scattering-Induced Attenuation of an Ultrasonic Beam in Austenitic Steel*, Journal of the Acoustical Society of America, Vol. 108, No. 2, pp. 580-587 (2000).

[9] AHMED S. & THOMPSON R.B., *Effect of Preferred Grain Orientation and Grain Elongation on Ultrasonic Wave Propagation in Stainless Steel*, Review of Progress in QNDE, Vol. 11, pp. 1999-2006 (1992).

[10] HIRSEKORN S., *Directional Dependence of Ultrasonic Propagation in Textured Polycrystals*, Journal of the Acoustical Society of America, Vol. 79, No. 5, pp. 1269-1279 (1986).

[11] HOSTEN B., *Reflection and Transmission of Acoustic Plane Waves on an Immersed Orthotropic and Viscoelastic Solid Layer*, Journal of the Acoustical Society of America, Vol. 89, No. 6, pp. 2745-2752 (1991).

[12] SEKI H., GRANATO A. & TRUELL R., *Diffraction Effects in the Ultrasonic Field of a Piston Source and their Importance in the Accurate Measurement of Attenuation*, Journal of the Acoustical Society of America, Vol. 28, No. 2, pp. 230-238 (1956).